sina-pub.ir

Colloids and Surfaces B: Biointerfaces 75 (2010) 179–185

Contents lists available at ScienceDirect

Colloids and Surfaces B: Biointerfaces

journal homepage: www.elsevier.com/locate/colsurfb

A sensitive DNA biosensor fabricated with gold nanoparticles/ploy (*p*-aminobenzoic acid)/carbon nanotubes modified electrode

Yuzhong Zhang[a,*], Jie Wang[a], Minglu Xu[b]

[a] College of Chemistry and Materials Science, Anhui Key Laboratory of Chemo-Biosensing, Anhui Normal University, Wuhu 241000, PR China
[b] Henan Institute of Science and Technology, Xinxiang 453003, PR China

ARTICLE INFO

Article history:
Received 25 June 2009
Received in revised form 4 August 2009
Accepted 18 August 2009
Available online 25 August 2009

Keywords:
DNA biosensor
Multi-walled carbon nanotubes
Gold nanoparticles
Electropolymerization
Electrochemical deposition

ABSTRACT

In this work, we fabricated a sensitive electrochemical DNA biosensor for the detection of target DNA. Aminobenzoic acid (ABA) was firstly electropolymerized on the surface of the glassy carbon electrode (GCE) modified with multi-walled carbon nanotubes with carboxyl groups (MWCNTs) by cyclic voltammetry (CV). Gold nanoparticles (AuNPs) were subsequently introduced to the surface of PABA–MWNTs composite film by electrochemical deposition mode. Probe DNA was immobilized on the surface of AuNPs through Au–S bond. Scanning electron microscopy (SEM), cyclic voltammetry (CV) and electrochemical impedance spectra (EIS) were used to investigate the film assembly process. Differential pulse voltammetry (DPV) was used to monitor DNA hybridization event by measurement of the intercalated adriamycin. Under the optimal conditions, the increase of reduction peak current of adriamycin was linear with the logarithm of the concentration of the complementary oligonucleotides from 1.0×10^{-12} to 5.0×10^{-9} M with a detection limit of 3.5×10^{-13} M. This DNA biosensor has a good stability and reproducibility.
Crown Copyright © 2009 Published by Elsevier B.V. All rights reserved.

1. Introduction

Sequence-specific detection of nucleic acid targets has become increasingly important in disease diagnostics, drug screening, epidemic prevention, and environmental protection [1,2]. Various techniques have been developed for the detection of target DNA, including radio-chemical, quartz crystal microbalance, and electrochemistry method. Among these techniques, electrochemical DNA sensors have attracted significant research interests, due to its high sensitivity, small dimensions and low cost. To date, a variety of approaches have been explored in electrochemical detection of DNA hybridization [3–6]. Such sensors are commonly accomplished by using electroactive indicators [7–11], through enzyme amplified recognition [12], redox tages covalently bond to single-stranded DNA oligomers [13–17], nanoparticle [18–20] and electroactive beads [21] amplified signal. Detecting technology of those sensors generally are DPV [22], EIS [23,24], anodic stripping voltammetry (ASV) [25,26], and chronocoulometry (CC) [27]. Recently, several reviews about this field have been reported [28–34].

As is well known, the immobilization of DNA probes onto electrode surfaces is one of the key steps toward DNA sensor development. It has been well demonstrated that the DNA sensor performance (e.g., sensitivity, selectivity, and stability) is highly dependent on properties of immobilized DNA probes. Several methods for immobilizing DNA probes onto electrode surface have been reported, including physical adsorption, cross-linking and electrochemical polymerization. Because electrochemical polymerization can control film thickness, permeation and charge transport characteristics by adjusting the electrochemical parameters. So the electrochemical polymerization is one of the promising approaches to immobilize DNA probes, such as poly(pyrrole) [24], and the polymers have been proven to be a very suitable matrix for biosensors with fast response time, high sensitivity and great versatility in analytical tools [35,36].

Carbon nanotubes (CNTs) are novel nanomaterials, which have been widely recognized as an ideal support for fabricating electrochemical sensors. The CNT-based sensors have shown good sensitivity and selectivity. Recently, composite materials based on integration of CNTs and polymers have gained growing interest because they possess the properties of each component with a synergistic effect. Jiao and co-works have fabricated several electrochemical DNA biosensor based on polymer–CNT composite film modified electrode, including PDDA/poly (2,6-pyridinedicarboxylic acid)-MWCNTs [37], Poly(L-lysine)/SWCNT film [38]. Previously, we fabricated DNA biosensor based on Ag_{nano}/PPAA/CNT film modified electrode [39]. This DNA biosensors show good selectivity and sensitivity.

p-Aminobenzoic acid (ABA) contains electron-rich N atom and high electron density of carbonyl group, and it is easy to be polymerized on glassy carbon electrode by CV. Jin and co-workers have ever applied poly (*p*-ABA) modified electrode to investigate an

* Corresponding author. Tel.: +86 553 3869303; fax: +86 553 3869303.
E-mail address: zhyz65@mail.ahnu.edu.cn (Y. Zhang).

0927-7765/$ – see front matter. Crown Copyright © 2009 Published by Elsevier B.V. All rights reserved.
doi:10.1016/j.colsurfb.2009.08.030

sina-pub.ir

experimental Parkinsonian animal model [40]. This polymeric film modified electrode has been used to detect dopamine in the present of ascorbic acid [41].

In the present work, we fabricated a sensitive DNA biosensor based on PABA/MWCNTs composite film modified electrode. First, ABA was electropolymerized on the surface of GCE modified with MWCNT by CV. Second, AuNPs was introduced to the surface of polymer–MWCNT by electrodeposition mode. Third, probe DNA was immobilized on the surface of AuNPs through Au–S bond. DPV was used to detect hybridization events using adriamycin as an electroactive indicator. The experiment result shows the increase of reduction peak current of adriamycin was linear with the logarithm of the concentration of the complementary oligonucleotides from 1.0×10^{-12} to 5.0×10^{-9} M with a detection limit of 3.5×10^{-13} M. The approach to probing DNA immobilization and hybridization with target oligonucleotides is illustrated in Schemes 1 and 2.

2. Experimental

2.1. Reagents

Adriamycin hydrochloride was obtained from the National Institute for the Control of Pharmaceutical and Biological Products (Beijing, China). *p*-Aminobenzoic acid was purchased from Guoyao Chemical Reagent Co. Ltd., and sodium dodecyl sulfate (SDS) was purchased from Alfa Aesar China Co. Ltd. (Tianjing, China). Multi-walled carbon nanotubes with carbonxyl acid (MWCNTs) (diameter 20–30 nm, length 30 mm, purity >95%) were obtained from Chengdu Institute of Organic Chemistry, Chinese Academy of Sciences, and used without further purification. The various oligonucleotides were purchased from Shanghai Sangon Bioengineering Technology & Services Co. Ltd. (Shanghai, China), and their sequences are as follows:

Probe oligonucleotides: SH-$(CH_2)_6$-5′-AAG CGG AGG ATT GAC GAC TA-3′.
Complementary oligonucleotides: 5′-TAG TCG TCA ATC CTC CGC TT-3′.
Non-complementary oligonucleotides: 5′-AAG CGG AGG ATT GAC GAC TA-3′.
Three-base mismatched oligonucleotides: 5′-TAG ACG TCA TTC CTC CCC TT-3′.

Stock solutions of oligonucleotides were prepared with 0.1 M PBS solution (pH 7.0) and stored in a freezer. All chemicals were of analytical grade and used without further purification. All solutions were prepared with twice-quartz-distilled water.

2.2. Instrumentation

CV and DPV experiments were performed on a CHI 660A electrochemical workstation (Shanghai Chenhua Instruments Co., China). A conventional three-electrode configuration was employed all through the experiment, which involved an interest working electrode, a platinum wire auxiliary electrode, and a saturated calomel electrode (SCE) reference electrode. All measurements were performed in a 10 ml electrolytic cell with 5 ml solutions, from which oxygen was removed by purging with high-purity nitrogen for 20 min, and a blanket of nitrogen was maintained over the solution during the measurements. All the measurements were carried out at room temperature. All potentials given in this article are referred to the SCE. The morphologies of MWCNTs, PABA/MWCNT, AuNPs/PABA/MWCNT were investigated with scanning electron microscopy [SEM, JEOLJSM-6700F].

EIS measurements were performed in the presence of 10 mM $K_3[Fe(CN)_6]/K_4[Fe(CN)_6]$ (1:1) mixture as a redox probe in the frequency range between 1 and 10^5 Hz at the formal potential of +0.15 V. The amplitude of the alternate voltage was 5 mV.

2.3. Preparation of ssDNA /Au_{nano}/PABA/MWCNTs modified electrode

Prior to modification, the bare GCE (3 mm in diameter, CH Instruments Inc.) was first polished to a mirror-like surface with gamma alumina suspensions (1.0, 0.25 and 0.05 μm, respectively). Then it was rinsed with double distilled water, and sonicated in ethanol and water for 3 min, respectively. Finally, the electrode was electrochemically cleaned from −1.2 to +1.2 V in pH 7.0 PBS for 10 circles to remove any remaining impurities.

MWCNTs (1 mg) were dispersed in 10 ml anhydrous ethanol with the aid of ultrasonic agitation to give a black suspension. Then a 10 μl aliquot of the suspensions was dropped onto the fresh surface of the GCE and dried naturally at room temperature to form MWCNTs film. Afterwards, it was immersed into water for 5 min to remove loosely adsorbed MWCNTs. The electropolymerization of ABA was performed by cyclic potential scanning from −1.5 to 2.5 V for 10 cycles with a scan rate of 100 mV s^{-1} in pH 7.0 PBS containing 2.0×10^{-3} M ABA on an MWNTs/GCE [41]. The obtained electrode was denoted as PABA/MWCNTs/GCE.

Gold electrochemical deposition was performed in 3.0×10^{-3} M $HAuCl_4$/0.1 M $NaNO_3$ solution with PABA/MWCNTs/GCE and electrodeposition time is 25 s at −200 mV (vs. SCE) [42]. The obtained electrode was denoted as Au_{nano}/PABA/MWCNTs/GCE.

Immobilization of the probe DNA is described as follows: 4 μl of 1.0×10^{-5} M probe DNA was dropped on the surface of Au_{nano}/PABA/MWCNTs/GCE, and it was then dried at 4 °C in a refrigerator. After that the probe modified electrode was immersed into 0.1% SDS solution for 10 min to remove the unimmobilized probe DNA. The probe modified electrode was denoted as ssDNA/Au_{nano}/PABA/MWCNTs/GCE.

2.4. Electrochemical detection of DNA hybridization

The hybridization reaction was performed by immersing the probe DNA modified electrode in 0.1 M PBS solution containing different concentrations of target DNA for 40 min at 37 °C. The hybridized electrode was next immersed into 0.1% SDS for 10 min to remove the unhybridized ssDNA. After that, it was immersed in a 0.1 M PBS solution containing 1.0×10^{-6} M adriamycin for 35 min at room temperature, followed by rinsing with water and pH 7.0 PBS for three times to remove physically absorbed adriamycin.

The DNA hybridization was assessed with the DPV peak current of intercalated adriamycin in pH 7.0 PBS. The concentration of target DNA was quantified by the reduction peak current (ΔI) of adriamycin, which was subtracted from the reduction peak current generated at the ssDNA/Au_{nano}/PABA/MWCNTs modified electrode. The DPV parameters were as follows: potential interval from −0.3 to −0.9 V; the amplitude, 100 mV; pulse width, 50 ms; sampling width, 0.0167 V; pulse period, 0.2 s; quiet time, 2 s.

3. Results and discussion

3.1. Electropolymerization of p-ABA at the MWCNTs/GCE

Fig. 1 shows repetitive voltammograms of 2.0×10^{-3} mol l^{-1} *p*-ABA in pH 7.0 PBS at the MWCNTs modified electrode. In the first scan, anodic peak (a) and cathodic peak (c) are observed with peak potential value at +1.47 and −0.80 V, respectively. From the second cycle on, anodic peak (b) appears with potential at +0.24 V. Then

sina-pub.ir

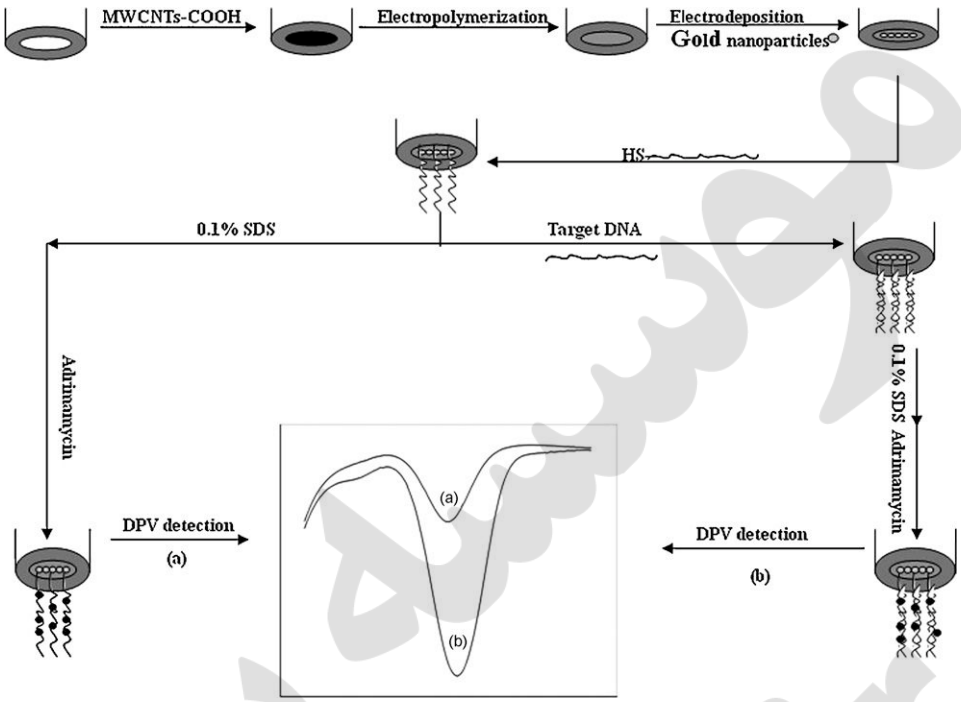

Scheme 1. Schematic illustrations of the immobilization and hybridization detection of probe DNA.

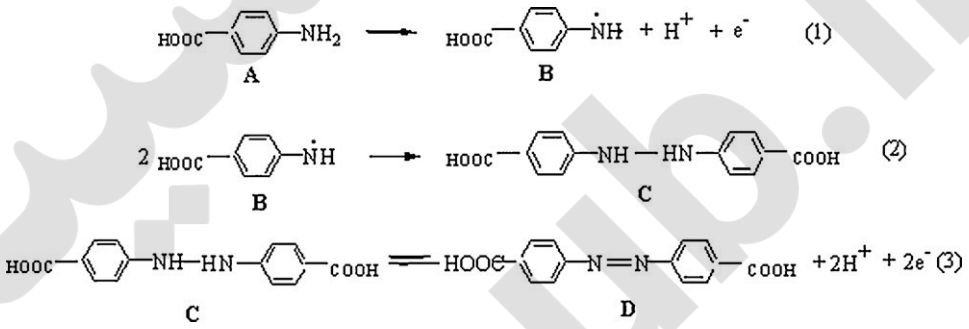

Scheme 2. The mechanism of ABA at MWCNT modified electrode.

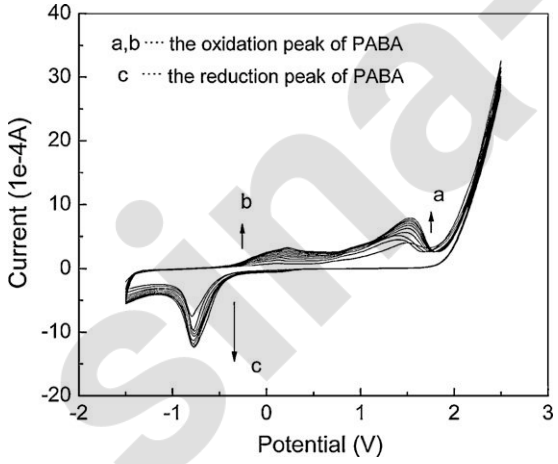

Fig. 1. Repetitive cyclic voltammograms of 2.0×10^{-3} mol l^{-1} *p*-ABA at the MWCNTs modified electrode. Terminal potential: +2.5 V; Initial potential: −1.5 V; Sensitivity: 1.0×10^{-4} A/V; Scan rate: 100 mV s^{-1}.

larger peaks at 1.47 or −0.80 V are observed obviously upon continuous scanning, reflecting the continuous growth of the film. These facts indicate *p*-PABA was deposited on the surface of MWCNTs by electropolymerization mode. A uniform adherent blue polymer film was formed on the GCE surface. After modification, the poly (*p*-PABA) film electrode was carefully rinsed with doubly distilled water, then stored in air and was prepared to use later. The electrochemical behavior of *p*-PABA at MWCNT was similar to the references [40,41]. The reaction mechanism may be described as following (Eq. (1)–(3)): *p*-PABA (A) was firstly oxidized to free radical (B) (Peak a); the free radical (B) combined together rapidly to hydrazobenzoic acid (C); then hydrazobenzoic acid (C) was oxidized to azobenzoic acid (D) (Peak b), and azobenzoic acid (D) reduced to hydrazobenzoic acid (C) (Peak c).

The SEM images of the MWCNTs, PABA/MWCNTs, and Au_{nano}/PABA MWCNTs film are shown in Fig. 2. From Fig. 2A, it can be seen that the MWCNTs were distributed very homogeneously on the GCE. After the ABA was electropolymerized on the surface of the MWCNTs/GCE, the amount of MWCNTs is lower, and the images are cloudily because MWCNTs is covered with a thin film of PABA (seen in Fig. 2B). After AuNPs were introduced to the surface of PABA/MWCNTs film, AuNPs can be observed obviously from Fig. 2C.

sina-pub.ir

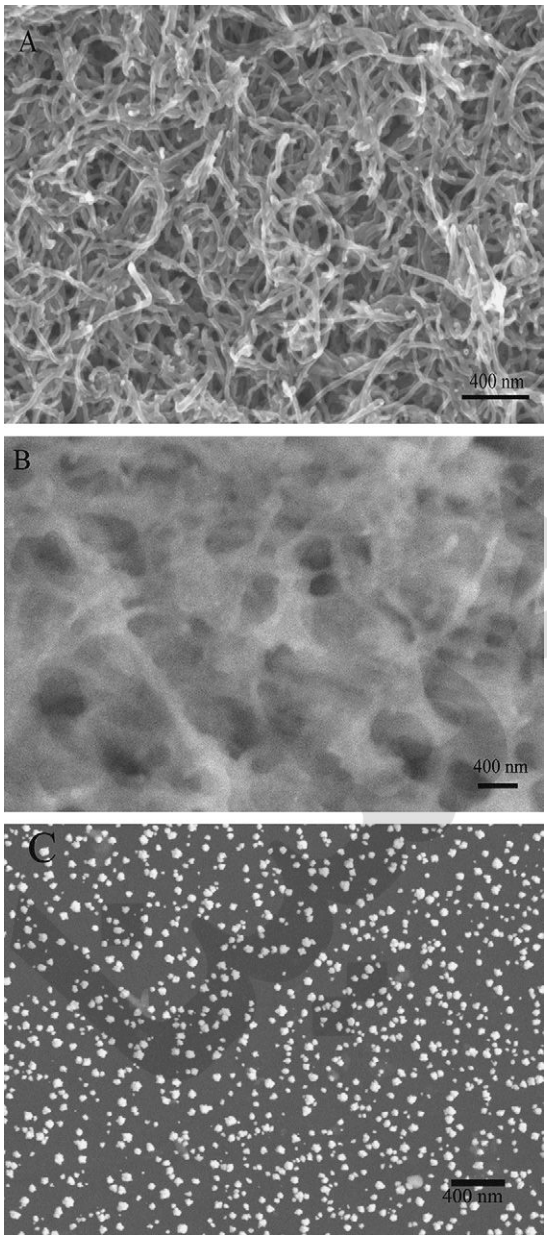

Fig. 2. SEM images of MWCNTs/GCE (A), PABA/MWCNTs/GCE (B), and Au_{nano}/PABA/MWCNTs /GCE (C).

3.2. Electrochemical impedance characterization of modified electrode

Fig. 3 shows the Nyquist plots of the sensing electrode responses at different stages in assembly process. Significant differences in the impedance spectra are observed during stepwise modification of the electrodes, when the MWCNTs was assembled on the GCE, the electron transfer resistance (R_{et}) decrease greatly (curve b) compared with that of the bare GCE (curve a). This may be attributed to the good promotion of MWCNTs to the interfacial electron transfer between the electrode and the electrolyte solution. When ABA was electropolymerized on the surface of MWCNTs/GCE, R_{et} increases (curve c). After AuNPs was introduced to electrode surface, the R_{et} decrease (curve d). When probe DNA was immobilized on electrode surface, the R_{et} obviously increases. The reason is that DNA is negatively charged and has electrostatic repulsion towards negatively charged $[Fe(CN)_6]^{3-/4-}$. Therefore, we can confirm that different species are immobilized on the surface of modified electrode from change of electron transfer resistance.

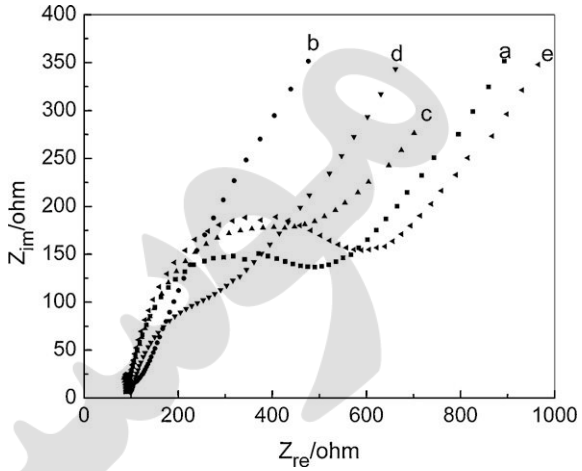

Fig. 3. Nyquist plots obtained at bare electrode (a); MWCNT modified electrode (b); PABA/MWCNT modified electrode (c); AuNPs/PABA/MWCNT modified electrode (d); ssDNA/AuNPs/PABA /MWCNT modified electrode (e); The supporting electrolyte was 0.1 M PBS (pH 7.0) containing 10.0 mM $K_4Fe(CN)_6/K_3Fe(CN)_6$ (1: 1).

3.3. Electrochemical characterization of adriamycin at the different modified electrodes

Fig. 4A compares DPVs of 1.0×10^{-6} M adriamycin at different modified electrodes. Fig. 4B shows corresponding histograms of the reduction peak currents. From Fig. 4A, we can observe that the peak currents of adriamycin is lower at the bare GCE (curve a) or Au_{nano}/GCE (curve b), and greatly enhanced at Au_{nano}/PABA modified electrode (curve c). Importantly, when MWCNTs was present, the peak current of adriamycin is remarkably improved (curve d). In addition, when the probe DNA immobilized on the surface of Au_{nano}/PABA/MWCNT/GCE, the peak current of adriamycin is obviously increased (curve e). The reason is that the negative charge phosphate backbone of DNA can absorbed positive charge adri-

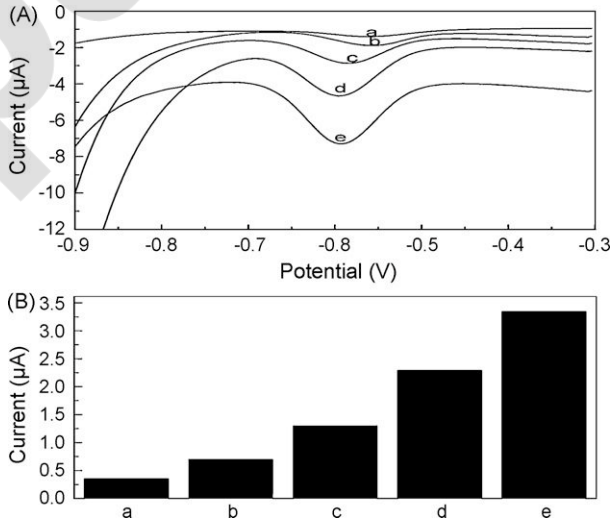

Fig. 4. (A) DPVs of 1.0×10^{-6} M adriamycin recorded at the bare GCE (a); the Au_{nano}/GCE (b); the Au_{nano}/PABA (c); the Au_{nano}/PABA/MWCNTs (d); the ssDNA/Au_{nano}/PABA/MWCNTs (e) modified GCE. Support electrolyte: 0.1 M PBS (pH 7.0); DPV measurement was performed at potential interval from -0.3 to -0.9 V. Experiment condition: the amplitude: 100 mV; pulse width: 50 ms; sampling width: 0.0167 V; pulse period: 0.2 s; quiet time: 2 s. (B) Corresponding histograms of the reduction peak current of adriamycin.

sina-pub.ir

amycin. This fact shows AuNPs can provide a well platform for the immobilization of probe DNA.

3.4. Optimization of DNA assay conditions

In order to obtain a much larger effective electrode surface area and provide a better environment for DNA immobilization and hybridization, electrodeposition time of gold was optimized by DPV. Fig. 5A shows the influence of deposition time on the peak current of adriamycin. It can be observed that the peak current increases significantly with increasing the deposition time from 0 to 20 s, keeps constant during 20 to 25 s, and decreases slightly after 25 s. So we select 25 s for the gold deposition time in this work.

Fig. 5B shows the relationship between the peak currents of adriamycin and the accumulation time. It can be seen the peak current increases significantly with accumulation time from 15 to 35 min, keep relatively constant in the range from 35 to 40 min, and decreased obviously after 40 min. So we select 35 min as accumulation time in this work.

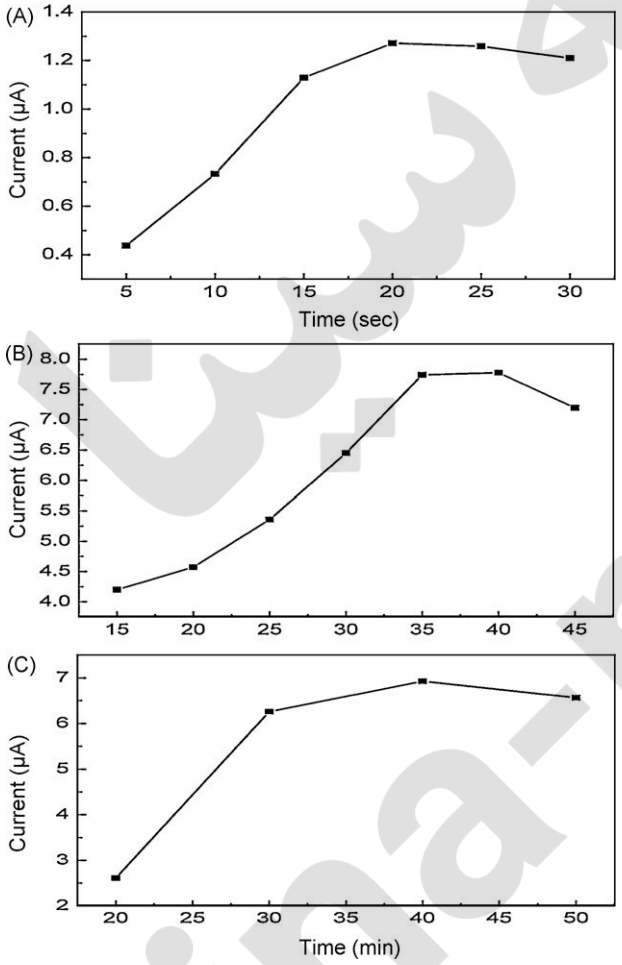

Fig. 5. (A) Effect of gold deposition time on DPV signals of adriamycin. Gold electrochemical deposition was performed in 3.0 mM $HAuCl_4$ at potential of −200 mV (vs. SCE) at various times (t = 5, 10, 15, 20, 25, 30 s). DPV measurement was performed in 0.1 M PBS (pH 7.0) containing 1.0×10^{-6} M adriamycin in the potential interval from −0.3 to −0.9 V. Experiment condition is the same as Fig. 4A. (B) Effect of accumulation time of adriamycin on DPV signals of adriamycin. The hybridized electrode was incubated in 0.1 M PBS (pH 7.0) containing 1.0×10^{-6} M adriamycin for various times (15, 20, 25, 30, 35 and 40 min). (C) Effect of DNA hybridization time on DPV signals of adriamycin. The ssDNA electrode was incubated in 0.1 M PBS (pH 7.0) containing 1.0×10^{-6} M complementary oligonucleotides at 37 °C for various times, and then the hybridized dsDNA electrode was incubated in 0.1 M PBS (pH 7.0) containing 1.0×10^{-6} M adriamycin for 35 min at room temperature. The DPV parameters were the same as in Fig. 4A.

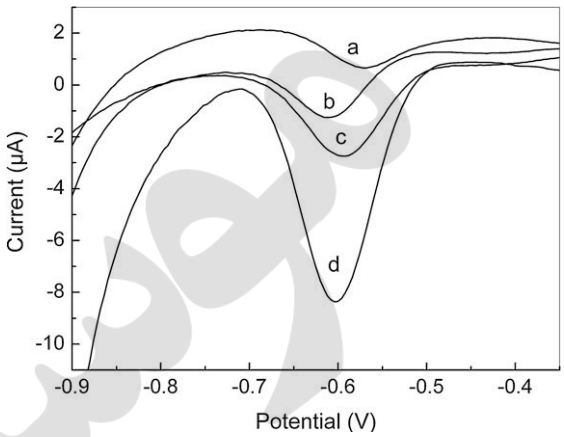

Fig. 6. DPVs of 1.0×10^{-6} M adriamycin recorded for the probe ssDNA/Au_{nano}/PABA/MWCNTs modified GCE (a) and after hybridization with 1.0×10^{-7} M non-complementary oligonucleotides (b); 1.0×10^{-7} M three-base mismatch oligonucleotides (c); 1.0×10^{-7} M complementary oligonucleotide sequence (d). Hybridization conditions and DPV parameters were the same as in Fig. 4A.

Fig. 5C shows the influence of the hybridization time on the peak current of adriamycin. From Fig. 5C, it can be seen that the peak current initially increases significantly with increasing the hybridization time from 20 to 30 min, then increases slowly from 30 to 40 min, and decreases after 40 min. Those results indicate that the hybridization reaction was dominantly completed after 40 min. From a view of the sensitivity and assay time, 40 min was chosen as the hybridization time in this work.

3.5. Selectivity of DNA biosensor

As a DNA biosensor, the selectivity is obviously a crucial factor to be considered. In this work, it was also evaluated using three-base mismatched and non-complementary DNA sequences. Fig. 6 displays DPVs of 1.0×10^{-6} M adriamycin for probe DNA (curve a), hybridized with its non-complementary sequence (curve b), three-base mismatch sequence (curve c), and complementary sequence (curve d). The peak currents of adriamycin are 2.247, 2.863, 4.375, and 8.631×10^{-6} A, respectively. Peak currents for non-complementary, three-base mismatch sequence are only 9.65% and 33.33% that of complementary sequence, respectively (the value is obtained according to equation: $\% = (I_{DS} - I_{SS})/(I_C - I_{SS})$, I_{DS}, peak current of adriamycin for non-complementary or three-base mismatch DNA; I_{SS}, peak current of adriamycin for probe DNA; I_C, peak current of adriamycin for complementary sequence). These results show that the fabricated DNA biosensor can be used to selectively assay the different sequences target DNA.

3.6. Analytical performance

Under the optimal conditions, the analytical performance of the DNA biosensor was investigated using the immobilized probe DNA to hybridize with the different concentrations of the complementary sequence. Fig. 7 shows the DPVs records of intercalated adriamycin at various complementary oligonucleotides concentrations. From Fig. 7, it can be seen that the peak current (ΔI) increases with the concentration of the complementary oligonucleotides increased and it is linear with the logarithm of the concentration of the complementary oligonucleotides in the range from 5.0×10^{-9} to 1.0×10^{-12} M. The regression equation is ΔI (μA) = 1.292 log C_{DNA} + 16.50 (unit of C is M), and the regression

sina-pub.ir

Table 1
Comparison of analytical performances of several electrochemical DNA sensors.

The DNA sensor	Detect technique	Linear detection range (nM)	Limit (nM)	Hybridization time (min)	Reference
DNA/Ag_{nano}/PPAA/ MWCNTs-COOH/GCE	DPV	0.009–9.0	3.2×10^{-3}	60	[39]
DNA/PICA/GCE	CV	3.34–10.6	0.094	45	[43]
DNA/Au_{nano}/cys/PGA	DPV	0.09–4.8	0.042	20	[44]
PolyPyrrole/ssDNA/ MCNTs paste electrode	DPV	0.1–1.0	8.5×10^{-3}	30	[45]
DNA/Au_{nano}/PLL/GCE	CC	$25–10^{-4}$	3.2×10^{-3}	40	This work

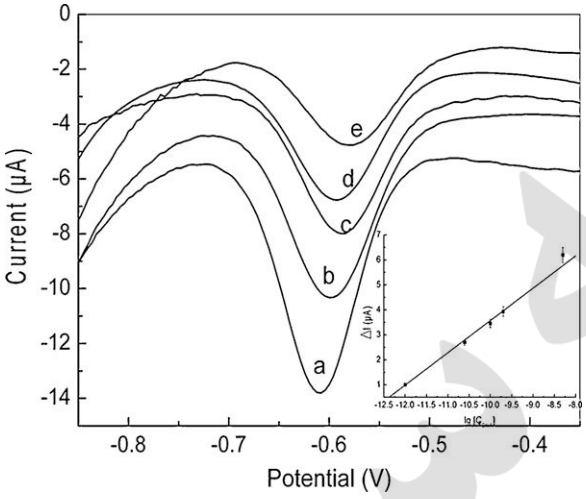

Fig. 7. The DPV response of the intercalated adriamycin recorded for the ssDNA/Au_{nano}/PABA/MWCNTs modified GCE that hybridized with various concentrations of complementary oligonucleotides: (a) 5.0×10^{-9} M; (b) 2.0×10^{-10} M; (c) 1.0×10^{-10} M; (d) 2.5×10^{-11} M; (e) 1.0×10^{-12} M. Inset: increase of peak current (ΔI) vs. logarithm of concentration of complementary oligonucleotides. DPV parameters were the same as in Fig. 4A.

coefficient (R) of the linear curve was 0.9979. The detection limit is 3.5×10^{-13} M (S/N = 3).

The linear range and detection limit of various electrochemical DNA sensors are shown in Table 1. From Table 1, a lower limit of detection and a wider linear range can be obtained by using the proposed sensor. In a word, the proposed DNA sensor has good analytical performances for the specific sequences of DNA detection.

3.7. Stability, reusability and reproducibility of DNA biosensor

The reproducibility and stability of this DNA sensor were investigated. If it was stored in the refrigerator at 4 °C and test after 3 days, no apparent change was observed in peak currents of adriamycin. The result indicates that the proposed DNA sensor has good stability.

The reusability of the DNA biosensor is investigated by immersing hybridized electrodes in hot water (80 °C) for 5–8 min, to completely remove hybridized DNA via thermal denaturation. The renew sensor was used to test response of 1.0×10^{-7} M target DNA, and found the fifth regenerated sensor has 93.0% response of the initial sensor (initial: 8.701×10^{-6} A, final: 8.091×10^{-6} A). This result indicates the proposed DNA biosensor has good reusability.

The reproducibility of the DNA sensor was also investigated as follows: Three DNA sensors were fabricated independently under the same conditions and are used to detect 1.0×10^{-7} M complementary oligonucleotides, respectively. The reduction peak current of adriamycin are 9.007, 8.635, and 8.256×10^{-6} A, respectively. The average value is 8.633×10^{-6} A, and the relative standard deviation (RSD) is 4.35%.

4. Conclusions

In conclusion, the present study has introduced a strategy for DNA hybridization detection by employing AuNPs/PABA/MWCNTs-COOH modified electrode. The experimental results show the DNA sensor has fast response, easy fabrication, and can detect three-base mismatched DNA sequence.

Acknowledgment

We thank the National Nature Science Foundation of China (No. 20675002), which financially supported this work.

References

[1] F.S. Nolte, B. Metchock, J.E. McGowan, A. Edwards, O. Okwumabua, C. Thurmond, P.S. Mitchell, B. Plikaytis, T. Shinnick, J. Clin. Microbiol. 31 (1993) 1777–1782.
[2] K. Senda, Y. Arakawa, K. Nakashima, H. Ito, S. Ichiyama, K. Shimokata, N. Kato, M. Ohta, Antimicrob. Agents Chemoth. 40 (1996) 349–353.
[3] T.G. Drummond, M.G. Hill, J.K. Barton, Nat. Biotechnol. 21 (2003) 1190–1199.
[4] J. Wang, X.J. Zhang, C. Parrado, G. Rivas, Electrochem. Commun. 1 (1999) 197–202.
[5] S.L. Pan, L. Rothberg, Langmuir 21 (2005) 1022–1027.
[6] J. Zhang, S.P. Song, L.Y. Zhang, L.H. Wang, H.P. Wu, D. Pan, C.H. Fan, J. Am. Chem. Soc. 128 (2006) 8575–8580.
[7] Y. Jin, X. Yao, Q. Liu, J.H. Li, Biosen. Bioelectron. 22 (2007) 1126–1130.
[8] X.H. Lin, P. Wu, W. Chen, Y.F. Zhang, X.H. Xia, Talanta 72 (2007) 468–471.
[9] H.L. Qi, X.X. Li, P. Chen, C.X. Zhang, Talanta 72 (2007) 1030–1035.
[10] H.C.M. Yau, H.L. Chan, M. Yang, Biosens. Bioelectron. 18 (2003) 873–876.
[11] Y.Z. Zhang, H.Y. Ma, K.Y. Zhang, S.J. Zhang, J. Wang, Electrochim. Acta 54 (2009) 2385–2391.
[12] G. Liu, Y. Wan, V. Gau, J. Zhang, L.H. Wang, S.P. Song, C.H. Fan, J. Am. Chem. Soc. 130 (2008) 6820–6825.
[13] A. Merkoci, M. Aldavert, S. Marın, S. Alegret, Trends Anal. Chem. 24 (2005) 341–349.
[14] J. Wang, J.H. Li, A.J. Baca, J.B. Hu, F.M. Zhou, W. Yan, D.W. Pang, Anal. Chem. 75 (2003) 3941–3945.
[15] C.H. Fan, K.V.W. Plaxco, A.J. Heeger, PNAS 100 (2003) 9134–9137.
[16] Y.L.N.N. Zhu, P. Yu, L.Q. Mao, Analyst 133 (2008) 1256–1260.
[17] H. Cai, N.N. Zhu, Y. Jing, P.G. He, Y.Z. Fang, Biosens. Bioelectron. 8 (2003) 1311–1319.
[18] M.T. Castaneda, S. Alegret, Electroanalysis 19 (2007) 743–753.
[19] X.L. Zhu, K. Han, G.X. Li, Anal. Chem. 78 (2006) 2447–2449.
[20] Z. Chang, H. Fan, K. Zhao, M. Chen, P.G. He, Y.Z. Fang, Electroanalysis 20 (2008) 131–136.
[21] J. Wang, R. Polsky, A. Merkoct, K.L. Turner, Langmuir 19 (2003) 989–991.
[22] H.Y. Ma, L.P. Zhang, Y. Pan, K.Y. Zhang, Y.Z. Zhang, Electroanalysis 20 (2008) 2127–2133.
[23] C.M. Li, C.Q. Sun, S. Song, V.E. Choong, G. Maracas, X.J. Zhang, Front. Biosci. 10 (2005) 180–186.
[24] Y. Xu, X.Y. Ye, L. Yang, P.G. He, Y.Z. Fang, Electroanalysis 18 (2006) 1471–1478.
[25] J. Wang, G.D. Liu, A. Merkoci, J. Am. Chem. Soc. 125 (2003) 3214–3215.
[26] J. Wang, D. Xu, A.N. Kawde, R. Polsky, Anal. Chem. 73 (2001) 5576–5581.
[27] K.C. Hu, D.X. Lan, X.M. Li, S.S. Zhang, Anal. Chem. 80 (2008) 9124–9130.
[28] C.H. Fan, K.W. Plaxco, A.J. Heeger, Trends Biotechnol. 23 (2005) 186–192.
[29] A. Erdem, Talanta 74 (2007) 318–325.
[30] K.J. Odenthal, J.J. Gooding, Analyst 132 (2007) 603–610.
[31] A. Erdem, M. Ozsoz, Electroanalysis 14 (2002) 965–974.
[32] J. Wang, Anal. Chim. Acta 500 (2003) 247–257.
[33] H.X. Ju, H.T. Zhao, Front. Biosci. 10 (2005) 37–46.
[34] J.J. Gooding, Electroanalysis 14 (2002) 1149–1156.
[35] G.C. Yang, Y. Shen, M.K. Wang, H.J. Chen, B.F. Liu, S.J. Dong, Talanta 68 (2006) 741.
[36] K. Arora, N. Prabhakar, S. Chand, B.D. Malhotra, Anal. Chem. 79 (2007) 6152.
[37] T. Yang, W. Zhang, M. Du, K. Jiao, Talanta 75 (2008) 987–994.
[38] C. Jiang, T. Yang, K. Jiao, H.W. Gao, Electrochim. Acta 53 (2008) 2917–2924.

sina-pub.ir

[39] Y.Z. Zhang, K.Y. Zhang, H.Y. Ma, Anal. Biochem. 387 (2009) 13–19.
[40] F. Xu, M.N. Gao, L. Wang, G.Y. Shi, W. Zhang, L.T. Jin, J.Y. Jin, Talanta 55 (2001) 329–336.
[41] Y.Z. Zhang, G.Y. Jin, W.X. Cheng, S.P. Li, Front. Biosci. 10 (2005) 23–29.
[42] A.X. Li, F. Fang, Y. Ma, X.R. Yang, Biosens. Bioelectron. 22 (2007) 1716–1722.
[43] X.M. Li, J.P. Xia, S.S. Zhang, Anal. Chim. Acta 622 (2008) 104–110.
[44] P.G. He, L.M. Dai, Chem. Commun. 3 (2004) 348–349.
[45] N. Prabhakar, K. Arora, S.P. Singh, M.K. Pandey, H. Singh, B.D. Malhotra, Anal. Chim. Acta 589 (2007) 6–13.

موسسه سینا sina-pub.ir